Solutions to Problems

Chapter 1

1.1. a. A dipolar resonance structure has aromatic character in both rings and would be expected to make a major contribution to the overall structure.

b. The "extra" polarity associated with the second resonance structure would contribute to the molecular structure but would not be accounted for by standard group dipoles.

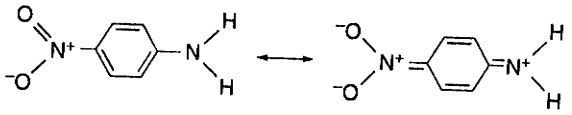

c. There are three major factors contributing to the overall dipole moments: (1) the σ-bond dipole associated with the C–O and C–N bonds; (2) the π-bond dipole associated with delocalization of π electrons from the heteroatom to the ring; and (3) the dipole moment associated with the unshared electron pair (for O) or N–H bond (for N). All these factors have a greater moment toward rather than away from the heteroatom for furan than for pyrrole. For pyrrole, the C–N π dipole should be larger and the N–H moment in the opposite direction from furan. These two factors account for the reversal in the direction of the overall dipole moment. The AIM charges have been calculated.

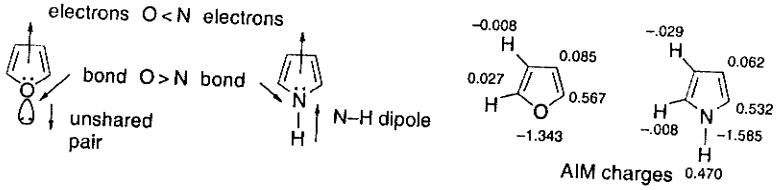

1.2. a. The nitrogen is the most basic atom.

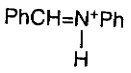

b. Protonation on oxygen preserves the resonance interaction with the nitrogen unshared electron pair.

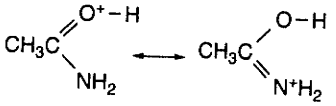

c. Protonation on nitrogen limits conjugation to the diene system. Protonation on C(2) preserves a more polar and more stable conjugated iminium system. Protonation on C(3) gives a less favorable cross-conjugated system.

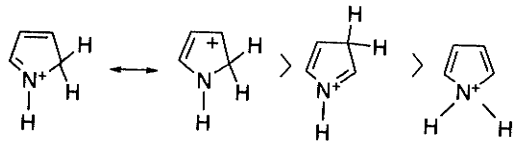

d. Protonation on the ring nitrogen preserves conjugation with the exocyclic nitrogen unshared electrons.

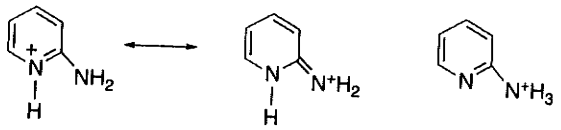

charge can be delocalized

charge is localized on exocyclic nitrogen

1.3. a. The dipolar resonance structure containing cyclopentadienide and pyridinium rings would be a major resonance contributor. The dipole moments and bond lengths would be indicative. Also, the inter-ring "double bond" would have a reduced rotational barrier.

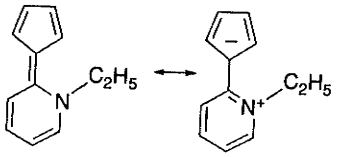

b. The dipolar oxycyclopropenium structure contributes to a longer C–O bond and an increased dipole moment. The C=O vibrational frequency should be shifted toward lower frequency by the partial single-bond character. The compound should have a larger pK_a for the protonated form, reflecting increased electron density at oxygen and aromatic stabilization of the cation.

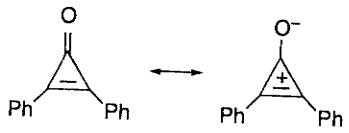

c. There would be a shift in the UV spectrum, the IR C=O stretch, and NMR chemical shifts, reflecting the contribution from a dipolar resonance structure.

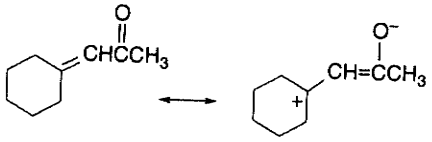

1.4. a. Amides prefer planar geometry because of the resonance stabilization. The barrier to rotation is associated with the disruption of this resonance. In MO terminology, the orbital with the C=O π^* orbital provides a stabilized delocalized orbital. The nonplanar form leads to isolation of the nitrogen unshared pair from the C=O system.

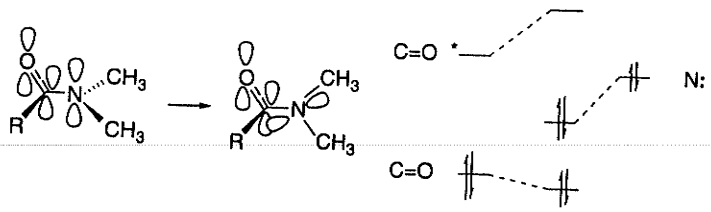

b. The delocalized form is somewhat more polar and is preferentially stabilized in solution, which is consistent with the higher barrier that is observed.

c. Amide resonance is reduced in the aziridine amide because of the strain associated with sp^2 hybridization at nitrogen.

The bicyclic compound cannot align the unshared nitrogen electron pair with the carbonyl group and therefore is less stable than a normal amide.

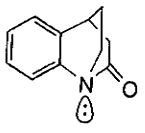

1.5. a. The site of protonation should be oxygen, since it has the highest negative charge density.

b. The site of reaction of a hard nucleophile should be C(1), the carbonyl carbon, as it has the most positive charge.

c. A soft nucleophile should prefer the site with the highest LUMO coefficient. The phenyl group decreases the LUMO coefficient, whereas an alkyl group increases it. Reaction would be anticipated at the alkyl-substituted carbon.

1.6. The gross differences between the benzo[b] and benzo[c] derivatives pertain to all three heteroatoms. The benzo[b] compounds are more stable, more aromatic, and less reactive than the benzo[c] isomers. This is reflected in both ΔH_f and the HOMO-LUMO gap. Also the greater uniformity of the bond orders in the benzo[b] isomers indicates they are more aromatic. Furthermore benzenoid aromaticity is lost in the benzo[b] adducts, whereas it increases in the benzo[c] adducts, and this is reflected in the TS energy and $\Delta H^{\ddagger}$. The order of $\Delta H^{\ddagger}$ is in accord with the observed reactivity trend O > NH > S. Since these dienes act as electron donors toward the dienophile, the HOMO would be the frontier orbital. The HOMO energy order, which is NH > S > O, does not accord with the observed reactivity.

1.7. The assumption of the C–H bond energy of 104 kcal/mol, which by coincidence is the same as the H–H bond energy, allows the calculation of the enthalpy associated with the center bond. Implicit in this analysis is the assumption that all of the energy difference resides in the central bond, rather than in strain adjustments between the propellanes and bicycloalkanes. Let BE_c be the bond energy of the central bond:

$$\Delta H = 2(\text{C–H}) - BE_c - \text{H–H} = 208 - BE_c - 104 = 104 - BE_c$$

$$BE_c[2.2.1]\text{propellane} = 104 - 95 = 5$$

$$BE_c[2.1.1]\text{propellane} = 104 - 73 = 31$$

$$BE_c[1.1.1]\text{propellane} = 104 - 39 = 65$$

This result indicates that while rupture of the center bond in [2.2.1]propellane is nearly energy neutral, the bond energy increases with the smaller rings. The underlying reason is that much more strain is released by the rupture of the [2.2.1]propellane bond than in the [1.1.1]propellane bond.

1.8. The various ΔH_{H2} values allow assigning observed ΔH_{H2} and ΔH_{isom} as in the chart below. Using the standard value of 27.4 kcal/mol for a *cis*-double bond allows the calculation of the heats of hydrogenation and gives a value for the "strain" associated with each ring. For example, the ΔH_{H2} of *cis*-cyclooctene is only 23.0 kcal/mol, indicating an increase of 27.4 – 23.0 = 4.4 kcal/mol of strain on going to cyclooctane. The relatively high ΔH_{H2} for *trans*-cyclooctene reflects the release of strain on reduction to cyclooctane. The "strain" for each compound is a combination of total strain minus any stabilization for conjugation. The contribution of conjugation can be seen by comparing the conjugated 1,3-isomer with the unconjugated 1,4- and 1,5-isomers of cyclooctadiene and is about 4 ± 1 kcal/mol. Since the "strain" for cyclooctatetraene is similar to the other systems, there is no evidence of any major stabilization by conjugation.

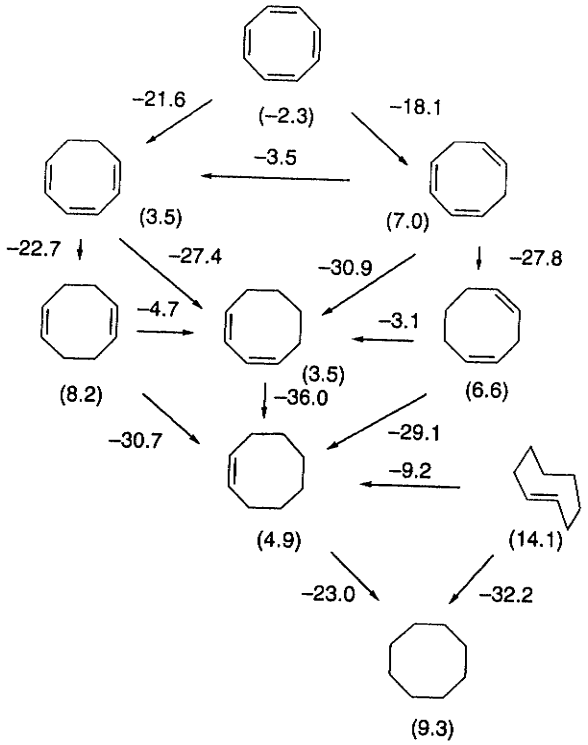

1.9. By subtracting the value for X=H from the other values, one finds the "additional" resonance stabilization associated with the substituent. There is some stabilization associated with the methyl and ethyl groups and somewhat more for ethenyl and ethynyl. This is consistent with the resonance concept that the unsaturated functional groups would "extend" the conjugation. The stabilization for amino is larger than for the hydrocarbons, suggesting additional stabilization associated with the amino group. The stabilizations calculated are somewhat lower than for the values for groups directly on a double bond.

1.10. The gas phase ΔG gives the intrinsic difference in stabilization of the anion, relative to the corresponding acid. The reference compound, CH_3CO_2H, has the highest value and therefore the smallest intrinsic relative stabilization. The differential solvation of the anion and acid can be obtained from p. 5 by subtracting the solvation of the acid from the anion. The numbers are shown below. The total stabilization favoring aqueous ionization, relative to acetic acid, is the sum of the intrinsic stabilization and the solvation stabilization. These tend to be in opposite directions, with the strongest acids having high intrinsic stabilization, but negative relative solvation.

X	Net solvation	Intrinsic	total	Δ
CH_3	77.58 − 7.86 = 69.72	345.94	345.94 − 69.72 = 276.22	–
H	77.10 − 8.23 = 68.87	342.49	342.49 − 68.87 = 273.62	−2.60
$ClCH_2$	70.57 − 10.61 = 59.96	333.50	333.50 − 59.96 = 273.54	−2.68
$NCCH_2$	69.99 − 14.52 = 55.47	327.66	327.66 − 55.47 = 272.19	−4.03
$(CH_3)_3C$	72.42 − 6.70 = 65.72	341.71	341.71 − 65.72 = 275.99	+0.23

We see that the final stabilization relative to acetic acid gives the correct order of pK_a. Interestingly, the solvation of the stronger acids is less than that of the weaker acids. This presumably reflects the effect of the stronger internal stabilization. These data suggest that intrinsic stabilization dominates the relative acidity for this series, with solvation differences being in the opposite direction.

1.11. These observations are the result of hyperconjugation between the nitrogen unshared electron pair and the axial C–H bonds. The chair conformation of the piperidine ring permits the optimal alignment. The weaker C–H bond reflects $N :\rightarrow \sigma^*$ delocalizations. The greater shielding of the axial hydrogen is also the result of increased electron density in the C–H bond. The effect of the axial methyl groups is one of raising the energy of the unshared electrons on nitrogen and stabilizing the radical cation.

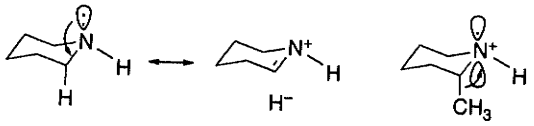

1.12. a–c. Each of these substitutions involves extending the conjugated system and results in an MO pattern analogous to allyl for fluoroethene and to butadiene for propenal and acrylonitile, respectively.

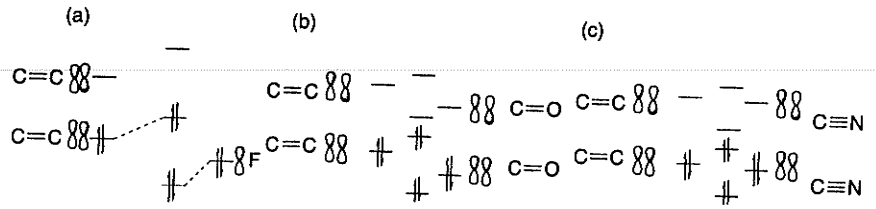

d. The addition of the methyl group permits $\sigma \rightarrow \pi^*$ and $\pi \rightarrow \sigma^*$ interactions that can be depicted by the π-type methyl orbitals. The σ orbitals can be depicted as the *symmetry-adapted* pairs shown. As a first approximation, one of each pair will be unperturbed by interaction of the adjacent π orbital because of the requirement that interacting orbitals have the same symmetry.

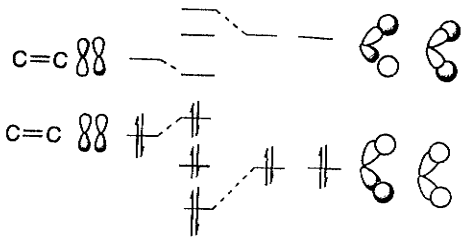

e–f. The substituents add an additional p orbital converting the conjugated system to a benzyl-like system. In the benzyl cation, the ψ_4 orbital is empty, resulting in a positive charge. In fluorobenzene, the p_z orbital on fluorine

will be conjugated with the π system and ψ_4 will be filled. This results in delocalization of some π-electron density from fluorine to the ring. The electronegative character of fluorine will place the orbitals with F participation at somewhat lower energy than the corresponding orbitals in the benzyl system. As a first approximation, the two benzene orbitals with nodes at C(1) will remain unchanged.

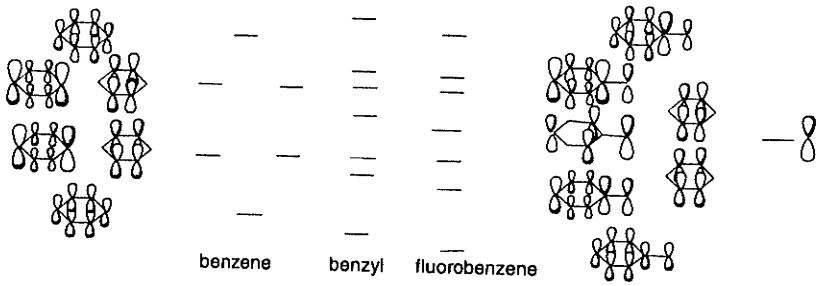

Comment. With the availability of suitable programs, these orbitals could be calculated.

1.13. a. The resonance interactions involve $\sigma \rightarrow \pi^*$ hyperconjugation in the case of methyl and $n \rightarrow \pi^*$ conjugation in the case of NH_2, OH, and F, as depicted below.

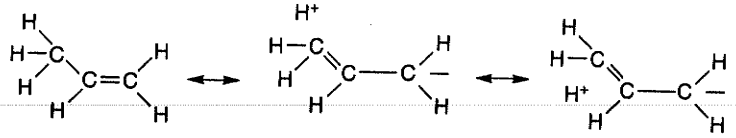

VB description of interaction with donor substituents

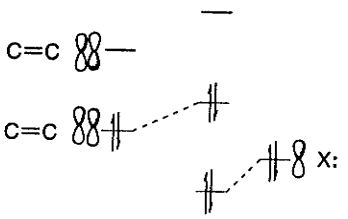

MO description of interaction with donor substituents

b. There are two major stabilizing factors at work. One is the π delocalization depicted for both the methyl group and heteroatoms. The order of this effect should be $NH_2 > OH > CH_3$, which is in accord with the observed order of the increase in stability. The other factor is the incremental polarity of the bonds, where an increment in stability owing to the electronegativity difference should occur. This should be in the order $F > OH > NH_2$, but this order seems to be outweighed by the effect of the π-electron delocalization.

c. The NPA charges are in qualitative agreement with the resonance/polar dichotomy. The electron density on the unsubstituted carbon C(2) increases, as predicted by the resonance structures indicating delocalization of the heteroatom unshared electron pair. The charge on the substituted carbon C(1) increases with the electronegativity of the substituent. As is characteristic (and based on a different definition of atomic charge), the AIM charges are dominated by electronegativity differences. There is some indication of the π-donor effect in that C(2) is less positive in the order $NH_2 < OH < F$.

1.14. a. In the strict HMO approximation, there would be two independent π and π^* orbitals, having energies that are unperturbed from the isolated double bonds, which would be $\alpha + \beta$ in terms of the HMO parameters.

b. There would now be four combinations. The geometry of the molecule tilts the orbitals and results in better overlap of the *endo* lobes. ψ_1 should be stabilized, whereas ψ_2 will be somewhat destabilized by the antibonding interactions between C(2) and C(6) and C(3) and C(5). ψ_3 should be slightly stabilized by the cross-ring interaction. The pattern would be similar to that of 1,3-butadine, but with smaller splitting of ψ_1 and ψ_2 and ψ_3 and ψ_4.

c. The first IP would occur from ψ_2, since it is the HOMO and the second IP would be from ψ_1. The effect of the donor substituent is to lower both IPs, but IP_1 is lowered more than IP_2. The electron-withdrawing substituent increases both IPs by a similar amount. The HOMO in the case of methoxy will be dominated by the substituted double bond, which becomes more electron rich as a result of the methoxy substituent. The cyano group reduces the electron density at both double bonds by a polar effect and conjugation.

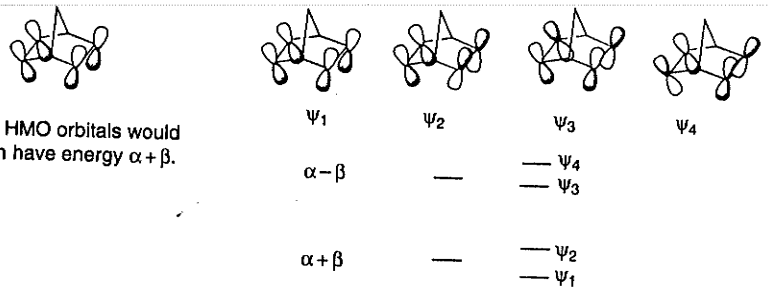

1.15. a. Since there are four π electrons in the pentadienyl cation, ψ_2 will be the HOMO.

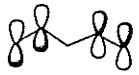

b. From the coefficients given, the orbitals are identified as ψ_2 and ψ_3, shown below. ψ_2 is a bonding orbital and is antisymmetric. ψ_3 is a nonbonding orbital and is symmetric.

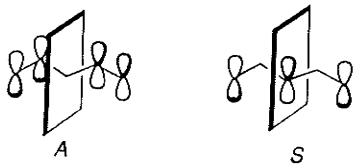

1.16. The positive charge on the benzylic position increases with the addition of the EWG substituents, which is consistent with the polarity of these groups. There is relatively little change at the ring positions. All the cations show that a substantial part of the overall cationic charge is located on the hydrogens. There is a decrease in the positive charge at the *para* position, which is consistent with delocalization to the substituent. All the structures show very significant bond length alterations that are consistent with the resonance structures for delocalization of the cation charge to the ring, especially the *para* position.

1.17. a. In terms of x the four linear homogeneous equations for butadiene take the form:

$$\begin{aligned} a_1 x + a_2 &= 0 \\ a_1 + a_2 x + a_3 &= 0 \\ a_2 + a_3 x + a_4 &= 0 \\ a_3 + a_4 x &= 0 \end{aligned}$$

where $x = -1.62, -0.618, 0.618$, and 1.62.

For ψ_1, $x = -1.62$, and we obtain

$$\begin{aligned} -1.62a_1 + a_2 &= 0 \\ a_1 - 1.62a_2 + a_3 &= 0 \\ a_2 - 1.62a_3 + a_4 &= 0 \\ a_3 - 1.62a_4 &= 0 \end{aligned}$$

The first equation yields

$$a_2 = 1.62a_1$$

Substitution of this value for a_2 into the second equation gives

$$a_1 - 1.62(1.62a_1) + a_3 = 0$$

or

$$a_3 = 1.62a_1$$

From the last equation, we substitute the a_3 in terms of a_1 and obtain

$$\begin{aligned} 1.62a_1 - 1.62a_1 &= 0 \\ a_4 &= a_1 \end{aligned}$$

We must normalize the eigenfunction:

$$a_1^2 + a_2^2 + a_3^2 + a_4^2 = 1$$

Making the appropriate substitutions gives

$$a_1^2 + 2.62a_1^2 + 2.62a_1^2 + a_1^2 = 1$$

$$a_1 = \frac{1}{\sqrt{7.24}}$$

$$a_1 = 0.372$$

$$a_2 = 0.602$$

$$a_3 = 0.602$$

$$a_4 = 0.372$$

and

$$\psi_1 = 0.372p_1 + 0.602p_2 + 0.602p_3 + 0.272p_4$$

To obtain the coefficients for ψ_2 we use the value of x, $x = -0.618$, and carry out the same procedure that is illustrated above. The results are:

$$a_2 = 0.618a_1$$

$$a_3 = -0.618a_1$$

$$a_4 = -a_1$$

and

$$a_1^2 + 0.382a_1^2 + 0.382a_1^2 + a_1^2 = 1$$

$$a_1 = \frac{1}{\sqrt{2.76}}$$

$$a_1 = 0.602$$

$$a_2 = 0.372$$

$$a_3 = 0.372$$

$$a_4 = 0.602$$

and

$$a_1^2 + 0.382a_1^2 + 0.382a_1^2 + a_1^2 = 1$$

$$a_1 = \frac{1}{\sqrt{2.76}}$$

$$a_1 = 0.602$$

$$a_2 = 0.372$$

$$a_3 = 0.372$$

$$a_4 = 0.602$$

$$\psi_2 = 0.602p_1 + 0.372p_2 - 0.372p_3 - 0.602p_4$$

Using the values $x = 0.618$ and 1.62, we repeat the same procedure for ψ_3 and ψ_4. The four eigenfunctions for butadiene are:

$$\psi_1 = 0.372p_1 + 0.602p_2 - 0.602p_3 - 0.372p_4$$
$$\psi_2 = 0.602p_1 + 0.372p_2 - 0.372p_3 - 0.602p_4$$
$$\psi_3 = 0.602p_1 + 0.372p_2 - 0.372p_3 - 0.602p_4$$
$$\psi_4 = 0.372p_1 + 0.602p_2 - 0.602p_3 - 0.372p_4$$

b.

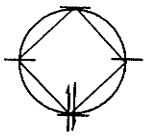

The MO diagram can be constructed using the Frost Circle. The energy of the occupied orbital is $\alpha + 2\beta$, so there is a stabilization of 2β, nominally the same as benzene, suggesting substantial stabilization for this ion.

c. The longest UV-VIS band should correspond to the HOMO-LUMO gap. For 1,3,5,7-octatetraene and 1,3,5-hexatriene the HMO orbitals are as follows:

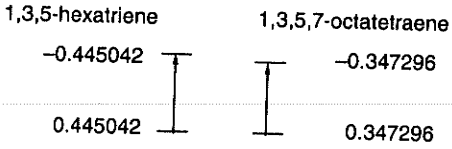

The energy gap decreases with the length of the conjugated system, and therefore the 1,3,5,7-octatetraene absorption should occur at longer wavelengths.

1.18. a. The additional strain in spiropentane relative to cyclopropane is due to the fact that there can be no relief of strain by rehybridization of the spiro carbon. By symmetry it is tetrahedral and maintains sp^3 hybridization.

b. These values provide further indication of the strain in spiropentane. The internal angle is close to that of an equilateral triangle (as in cyclopropane). The 137° value indicates considerable strain from the ideal 109° for an sp^3 carbon. This strain induces rehybridization in the C(2) and C(3) carbons.

c. Using 0.25 as the *s* character in the spiro carbon, we find the *s* character in the C(1)−C(2) bond to be $20.2 = 550(0.25)(x)$. The *s* character is 14.5%. For the C(2)−C(3) bond, $7.5 = 550(x^2)$. The fractional s character is 11.7%.

1.19. a. This reaction would be expected to be unfavorable, since cyclopropane is more acidic than methane. The increased *s* character of the cyclopropane C−H bond makes it more acidic. A gas phase measurement indicates a difference in ΔH of about 5 kcal/mol.

b. This comparison relates to the issue of whether a cyano group is stabilizing (delocalization) or destabilizing (polar) with respect to a carbocation (see p. 304). The results of a HF/3-21G calculation in the cited reference indicate a net destabilization of about 9 kcal/mol, in which case the reaction will be exothermic in the direction shown.

c. The polar effects of the fluorine substituents should strongly stabilize negative charge on carbon, suggesting that the reaction will be exothermic. An MP4SDTQ/6-31++(d,p) calculation finds a difference of ~ 45 kcal/mol.

1.20. a. Because of the antiaromaticity of the cyclopentadienyl cation (p. 31), the first reaction would be expected to be the slower of the two. The reaction has not been observed experimentally, but a limit of $< 10^{-5}$ relative to cyclopentyl iodide has been placed on its rate.

b. The cyclopropenyl anion is expected to be destabilized (antiaromatic). Therefore, K should be larger for the first reaction. An estimate based on the rate of deuterium exchange has suggested that the pK difference is at least 3 log units.

c. The second reaction will be the fastest. The allylic cation is stabilized by delocalization, but the cyclopentadienyl cation formed in the first reaction is destabilized.

1.21. The diminished double-bond character indicates less delocalization by conjugation in the carbene, which may be due to the electrostatic differences. In the carbocation, delocalization incurs no electrostatic cost, since the net positive charge of 1 is being delocalized. However in **B**, any delocalization has an electrostatic energy cost, since the localized sp^2 orbital represents a negative charge in the overall neutral carbene.

1.22. The results are relevant to a significant chemical issue, namely the stability of imines. It is known that imines with N-π-donor substituents, such as oximes (YX=HO) and hydrazones (YX = H_2N), are more stable to hydrolysis than alkyl (YX = H_3C). The classical explanation is ground state resonance stabilization:

$$\ddot{Y}\ddot{X}-N=CH_2 \longleftrightarrow \overset{+}{Y}X=N-CH_2^-$$

The stabilization is greatest for the F > OH > NH_2 series of substituents. The silyl group (ERG) is destabilizing, and the conjugated EWG groups are moderately stabilizing. The most significant structural change is in the bond angle, which implies a change in hybridization at nitrogen. The NPA charges show a buildup of charge on carbon for NH_2, OH, and F of about the same magnitude for each. This could result from the π delocalization. The charges on N are negative (except for F, where it is neutral) and seem to be dominated by the electronegativity of the substituent atom with the order being Si > C > N > O > F. These results indicate that as the substituent becomes more electronegative, the unshared pair orbital has more s character. (Results not shown here for X = Li and Na indicate that the lone pair is p in these compounds.) At least part of the stabilization would then be due to the more stable orbital for the unshared electron pair. A second factor in the stabilization may be a bond strength increment from the electronegativity difference between X and N.

1.23. The NPA charges indicate that the planar (conjugated) structures have characteristics associated with amide resonance. The oxygen charge in formamide is -0.710 in the planar form and -0.620 in the twisted form. For the NH_2 group, the charge is -0.080 in the planar form and -0.182 in the twisted form. These differences indicate more N to O charge transfer in the planar form. For 3-aminacrolein, the corresponding numbers are $O_{(planar)}$: -0.665, $O_{(twisted)}$: -0.625 and $NH_{2(planar)}$: -0.060, $NH_{2(twisted)}$: -0.149. These values indicate somewhat

less polarization associated with the (vinylic) resonance in this compound. For squaramide, the magnitude of the charges is similar $O(1)_{(planar)}$: −0.655; $O(1)_{(twisted)}$: −0.609 and $NH_{2(planar)}$: −0.001, $NH_{2(twisted)}$: −0.095. The differences in the ^{17}O chemical shifts and the rotational barrier also indicate greater resonance interaction in formamide than in 3-aminoacrolein and squaramide. The interaction maps show that the nitrogen is repulsive toward a positive charge in the planar forms, but becomes attractive in the twisted form. The attractive region is associated with the lone pair on the nitrogen atom in the twisted form.

Chapter 2

2.1. a. diastereomers; b. enantiomers; c. enantiomers; d. diastereomers; e. enantiomers; f. enantiomers.

2.2. a. *S*; $CH(C)_2 > CH_2CH(C)_2 > CH_2CH_2 > H$
b. *R*; Si > O > C > H
c. *R*; O > C=O > $C(C)_3$ > H
d. *R*; O > $C(C)_3$ > CH_2 > H
e. *S*; O > $C(C)_3C(C)_2H > C(C)_3C(C)H_2 > C(C)_2H$
f. *R*; N > $C(O)_3 > C(C)_2H > C(C)H_2$
g. *R*; O > $C(C)_3 > CH_3 >$: (electron pair)

2.3.

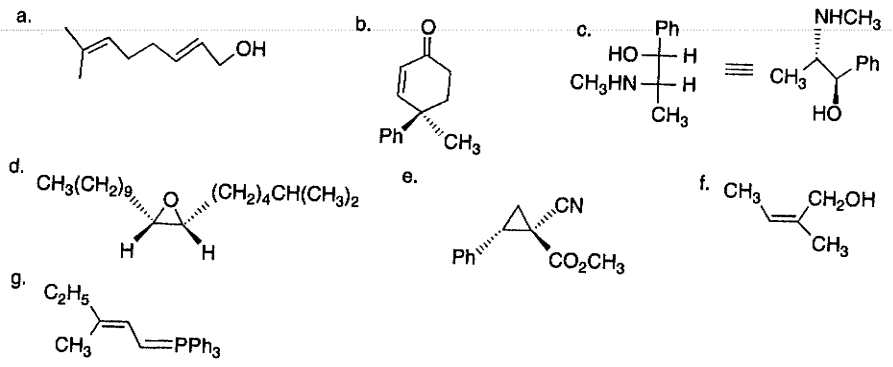

2.4.

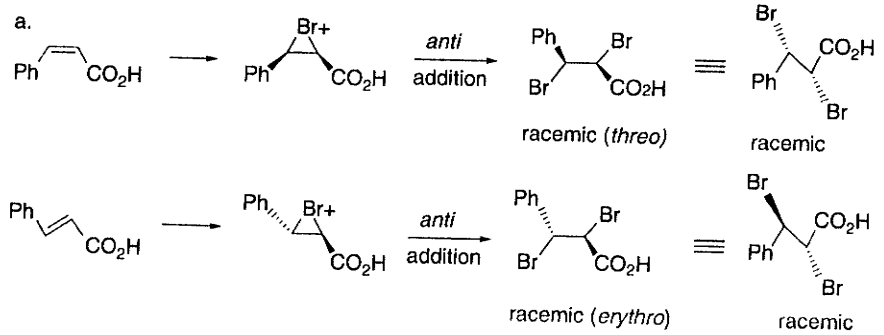

b.

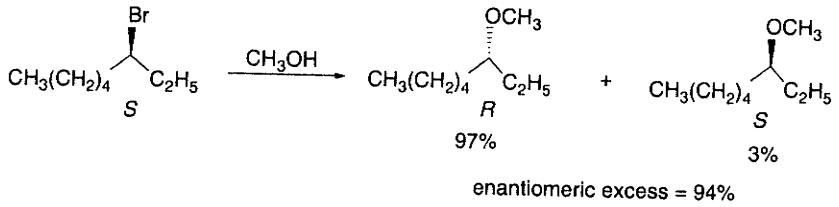

enantiomeric excess = 94%

c.

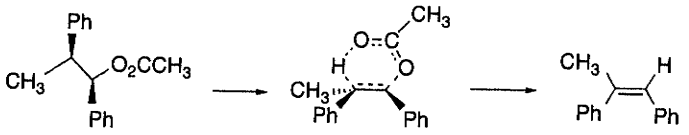

Z-isomer

d.

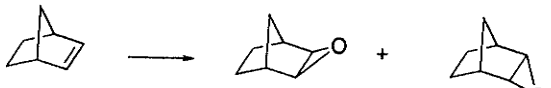

94% 6%

2.5. The solution to this problem lies in recognizing that there are steric differences for the phenyl group in the axial and equatorial conformations. In the equatorial position, the phenyl group can adopt an orientation that is more or less "perpendicular" to the cyclohexane ring, which minimizes steric interactions with the 2,6-equatorial hydrogens. In the axial conformation, the phenyl group is forced to rotate by about 90°, which adds to the apparent $-\Delta G_c$ for the phenyl group. When a 1-methyl substituent is present, the favorable "perpendicular" is no longer available and this destabilizes the equatorial orientation relative to phenylcyclohexane.

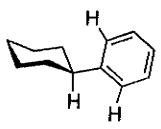

preferred conformation of *eq* 1-phenylcyclohexane

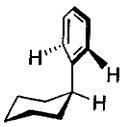

preferred conformation of *ax* 1-phenycyclohexane

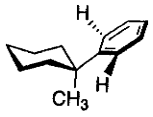

methyl group precludes preferred conformation and adds a destabilizing interaction with 2,6-*eq* hydrogens

Comment. This is a challenging question but can be approached effectively by MM modeling, as was done in the original and subsequent references.

2.6. As discussed on p. 148, the preferred conformation of acetone is the C−H/C=O eclipsed conformation. This is stabilized by a $\sigma \rightarrow \pi^*$ interaction. For 2-butanone the C(4)/C=O eclipsed is preferred, as discussed on p. 148 and illustrated by Figure 2.12. For 3-methyl-2-butanone, four distinct conformations arise. The maxima at 60° and 180° represent the CH_3/CH_3 eclipsed conformations, which give rise to a barrier of about 2.5 kcal/mol. This is somewhat less than for the CH_3/CH_3 eclipsed conformation of butane and presumably reflects the absence of additional H/H eclipsing. An analysis of the 3-methyl-2-butanone spectrum is available in Ref. 36, p. 149.

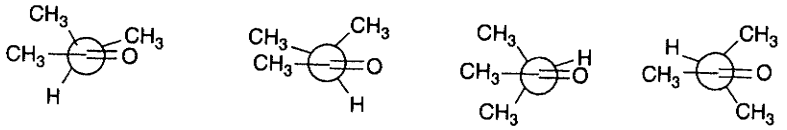

0°; 240° CH_3/C=O eclipsed

60°, 180°, staggered CH_3/CH_3 eclipsed

120°, H/C = O eclipsed

300°, staggered CH_3/H eclipsed

2.7. The stereochemistry of all of these reactions is governed by steric approach control.

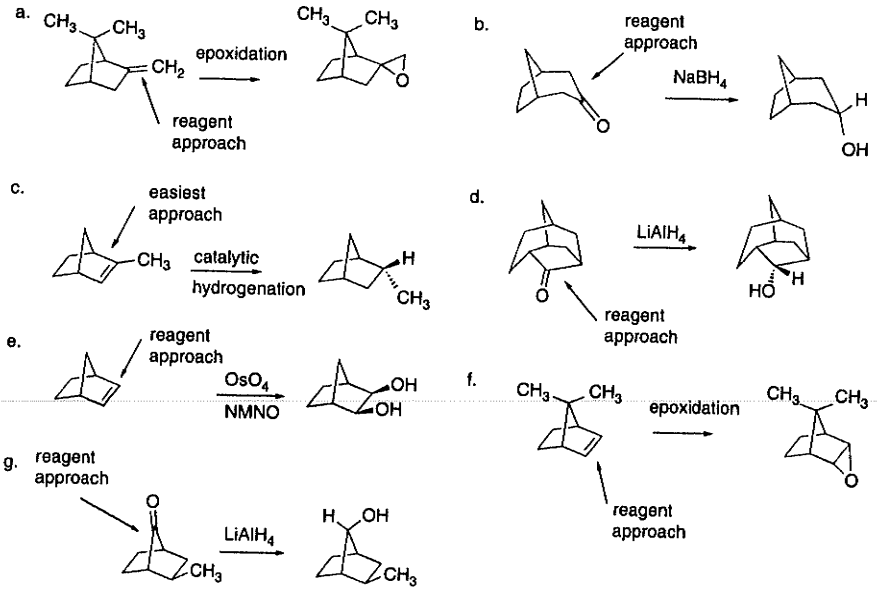

2.8. a, b. The conformers of 2-methylbutane differ by one "double" *gauche* interaction. The conformation of 2-methylbutane that avoids this interaction is favored by 0.9 kcal. There is good agreement between experimental and ab initio results. Surprisingly, the two conformations of 2,3-dimethylbutane are virtually equal in energy, by experimental, MM, and ab initio results. The qualitative "double" gauche argument fails in this case.

c. This is an example of the 3-alkyl ketone effect (p. 161), by which the conformational free energy of a 3-alkyl substituent is smaller than that in cyclohexane. The ΔG_c has been estimated as 0.55 kcal/mol.

Comment. Assuming availability of a suitable program, this question can framed as an exercise to calculate and compare the energies of the two conformations of each compound.

2.9. An estimate can be made by assuming additive ΔG_c and adding an increment (3.7 kcal/mol) for 1,3-diaxial interactions between methyl groups. The reference takes a somewhat different approach, summing *gauche* interaction terms to estimate the energy differences.

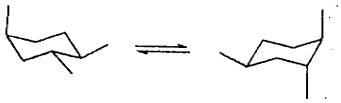

$-\Delta G = 3.4 - 1.7 = 1.7$

$-\Delta G = 3.4 - 1.7 - 3.7 = 5.4$

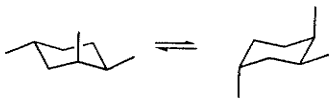

$-\Delta G = 3.4 - 1.7 = 1.7$

$-\Delta G = 3.7 + 3.4 - 1.7 = 5.4$

Comment. This problem would be amenable to an MM approach.

2.10. The conformation equilibria shown below have been measured.

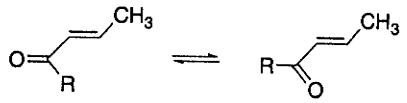

R	K
CH_3	0.45
C_2H_5	0.79
C_3H_7	1.00
i-C_4H_9	1.22
i-C_3H_7	2.3
t-C_4H_9	>100

The trend is a rather modest increase with size for the primary groups through isobutyl. There is a slightly larger change with the secondary isopropyl group, followed by a very large factor favoring the *s-cis* conformer for *t*-butyl. The very large increase on going to *t*-butyl occurs because there is no longer a hydrogen that can occupy the position eclipsed with the β-C–H in the *s-trans* conformation.

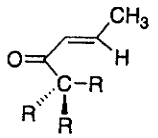

2.11. The product stereochemistry can be predicted on the basis of the Felkin model.

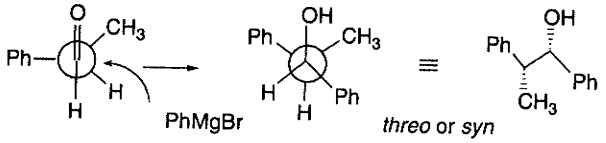

threo or *syn*

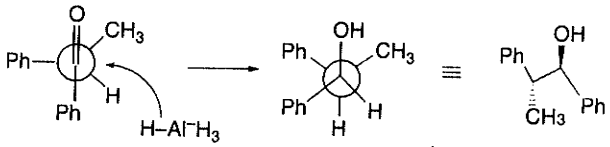

erythro or *anti*

Comment. The reference is an early formulation of Cram's rule and uses an alternative conformation of the reactant.

2.12. The α, β-double bond is held in proximity to the catalyst center by the acetamido substituent, while the γ, δ-double bond is not brought near the coordination center.

2.13.

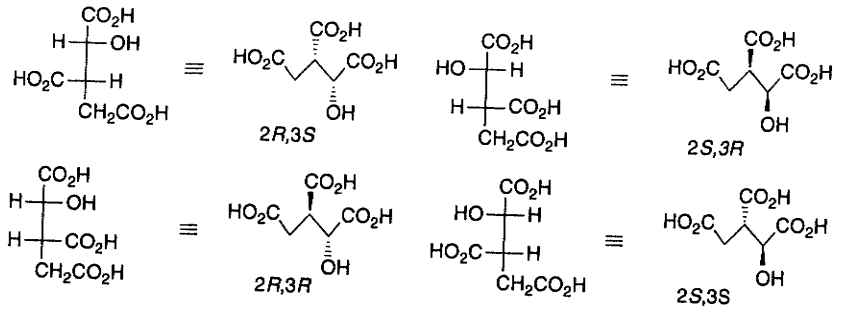

2.14. a.

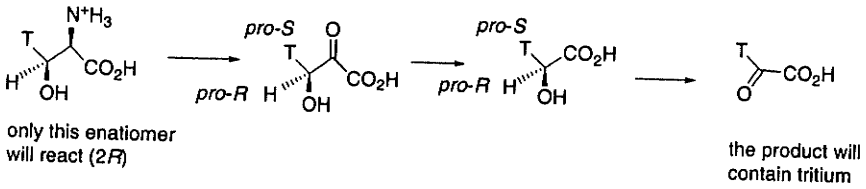

b.

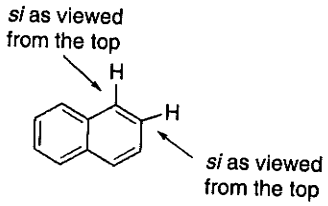

c. The reaction proceeds with retention of configuration at C(3). Inversion occurs at C(2).

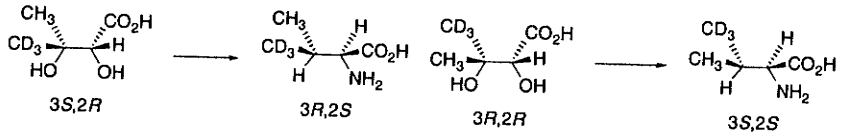

d.

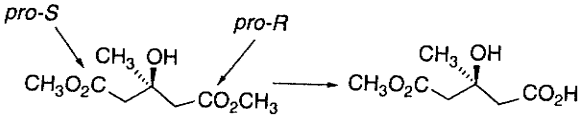

2.15. An achiral tetramer with a center of symmetry results if the two enantiomeric dimers nonactic acids are combined in a structure that contains a center of symmetry.

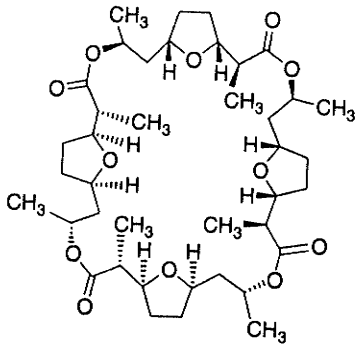

2.16. a. (a) The *cis* isomer is achiral while the *trans* isomer is chiral. The chirality of the *trans*-substituted ring system makes the benzyl hydrogens *diastereotopic* and nonequivalent. This results in the observation of geminal coupling and the appearance of an AB quartet. (b) Hyperconjugation with the nitrogen lone pair moves axial hydrogens to high field in piperidines. The *trans* isomer has one equatorial hydrogen, which appears near 2.8 ppm. In the *cis* isomer, only axial hydrogens are present and they appear upfield of the range shown.

b. Isomer **A** is the *cis,cis*-2,6-dimethyl isomer. The benzyl singlet indicates that there is no stereogenic center in the ring and the relatively narrow band at 3.4 indicates that there is only eq-ax coupling to the C(1) hydrogen. Isomer **B** is the *trans, trans*-2,6-dimethyl isomer. The benzyl singlet indicates an achiral structure but now the larger ax-ax coupling that would be present in this isomer is seen. Isomer **C** is the chiral *cis, trans*-2,6-dimethyl isomer. The AB quartet pattern of the benzyl hydrogens indicates that the ring system is the chiral *cis, trans* isomer. The splitting of the signal at 3.0 is consistent with one equatorial and one axial coupling.

2.17. The data allows calculation of $-\Delta G_c$. The interpretation offered in the reference is that hydrogen-bonding solvents (the last two entries) increase the effective size of the hydroxy group. The potential donor solvents dimethoxyethane and tetrahydrofuran seem to have little effect.

2.18. This result seems to be due to $\pi \rightarrow \sigma^*$ and $\sigma \rightarrow \pi^*$ hyperconjugation between the oximino and chloro substituents. Since hyperconjugation is also present in the ketone, the issue is raised as to why the oximino ethers are more prone to the diaxial conformation. The fact that the oximino ethers adopt the diaxial conformation indicates that the hyperconjugative stabilization is greater for the oximes than the ketones. This implies that the $\pi \rightarrow \sigma^*$ component must be dominant, since a greater donor capacity is anticipated for the oxime ethers.

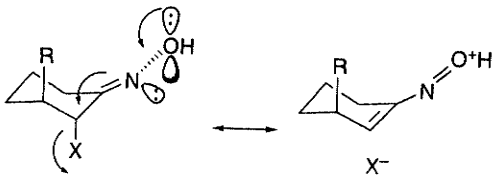

Comment. This question is amenable to MO analysis of the relative energies of the conformers and to NPA charge transfer analysis.

2.19. There is a significant barrier to rotation at the biaryl bond and this gives rise to the temperature dependence as well as introducing a stereogenic feature. In the *trans* isomer **19-A**, the two methyl groups are equivalent but the two conformers are *diastereomers*, and therefore not of equivalent energy. This is evident in the low-temperature spectrum from the unequal ratio. In the *cis* isomer **19-B**, the two conformations are enantiomeric but the methyl groups are nonequivalent. In the high-temperature spectrum, the nonequivalent signals are averaged.

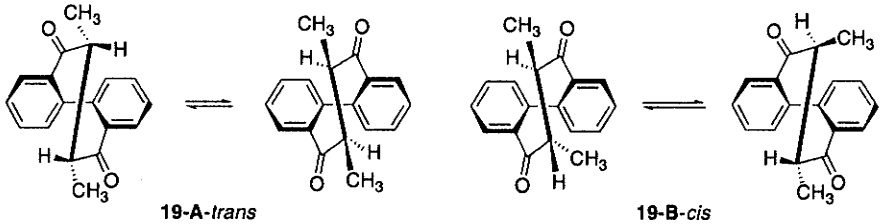

19-A-*trans* **19-B**-*cis*

2.20. The thermal isomerization of the alcohol involves a conformational change that allows the two aryl ring to "slip" by one another. This generates a diastereomer. Oxidation of the diastereomer then leads to the enantiomer of **20-B**.

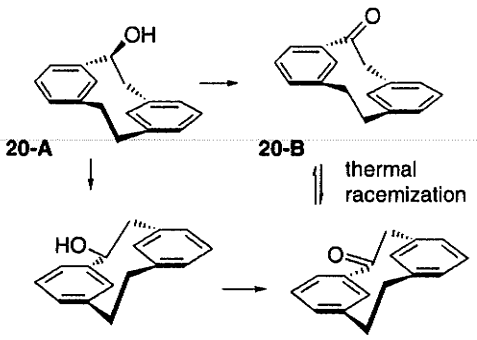

20-A **20-B**

2.21. Product **21-A** is a straightforward oxazoline derivative. Specifying the *R* configuration of the new stereogenic center should be possible on steric grounds. Product **21-B** is the achiral *meso* dimer. According to the reference, other epimeric dimers are 8–15 kcal/mol higher in energy on the basis of MNDO calculations.

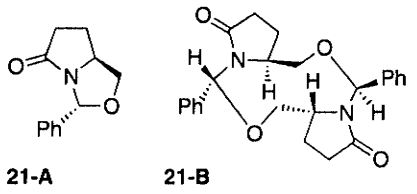

21-A **21-B**

The structure of **21-B** can be assigned on the basis of its dimeric composition, and recognition that it must have an achiral structure. Note that **21-B** is achiral as the result of a center of symmetry.

2.22. The major factor appears to be dipole-dipole repulsion between the C–X and C=O bond, which is at a maximum at 0°. This repulsion is reduced somewhat

in a more polar environment, accounting for the shift toward more of the *syn* conformation. There does not seem to be stabilization of the 90° conformation, which would presumably optimize C-X → π* hyperconjugation. The anomalous behavior of the nitro group is attributed to the somewhat different spatial orientation of the substituent.

2.23. a. The stereoselectivity is consistent with a chelated TS.

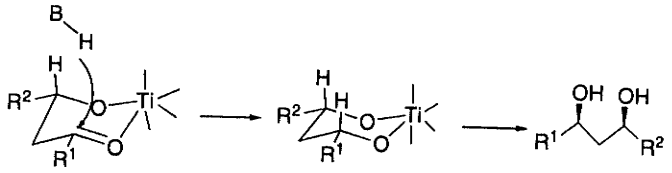

b. The observed stereoselectivity is consistent with a Felkin-Ahn model.

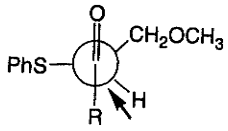

2.24. Application of the oxazaborolidine (p. 196) and $(Ipc)_2BCl$ (p. 194) models correctly predict the *R* configuration of the chiral center.

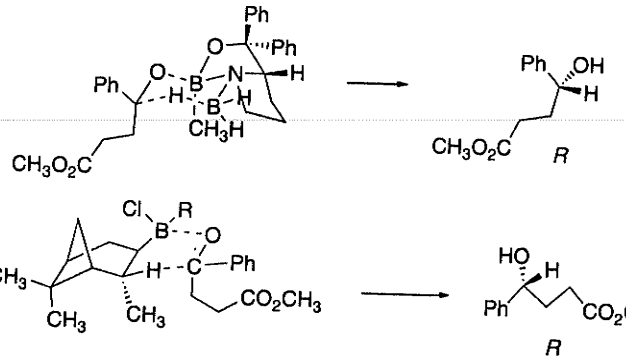

2.25. a. The two methyl groups are enantiotopic.

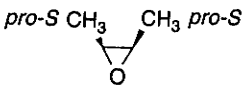

b. The two methyl groups are enantiotopic.

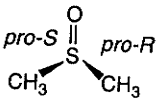

c. The methyls in the *i*-propyl group are diastereotopic.

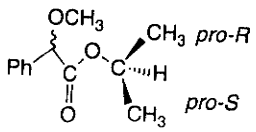

d. The two methyl groups are diastereotopic.

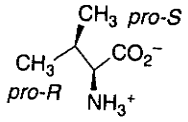

e. Both the benzyl and glycyl methylene hydrogens are diastereotopic.

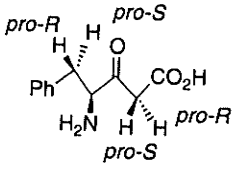

f. The ethoxy methylenes hydrogens are diastereotopic. The bromomethylene hydrogens are enantiotopic.

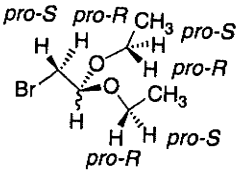

2.26. (a) chiral; (b) chiral, but note that inversion of the configuration of the methyl groups on one ring would give a molecule with a center of symmetry; (c) chiral; (d) achiral, plane of symmetry dissecting any ring and a ring junction; (e) achiral, center of symmetry and a plane of symmetry; (f) chiral; (g) chiral by virtue of helicity; (h) chiral; (i) chiral; (j) chiral; (k) chiral; (l) achiral, plane of symmetry aligned with the two C=O bonds; (m) chiral.

2.27. The following predictions are made by fitting the alkenes to the TS model in Figure 2.27.

(a) DHQD (*R*); DHQ (*S*)
(b) DHQD (*S*); DHQ (*R*)
(c) DHQD (*R*,*R*); DHQ (*S*,*S*)
(d) DHQD (*R*,*R*); DHQ (*S*,*S*)

2.28. a. The TS model on page 196 predicts *R* configuration.

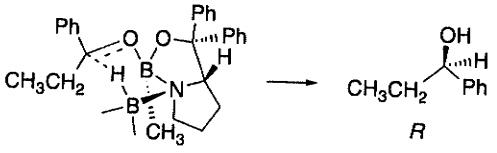

b. The TS model on page 194 predicts *R* configuration.

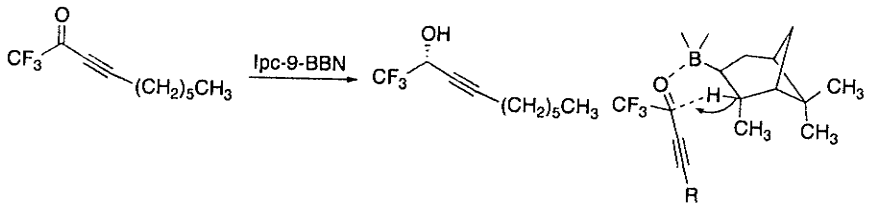

c. The empirical predictive scheme on p. 198 predicts that the 2*R*,3*S*-epoxide will be formed.

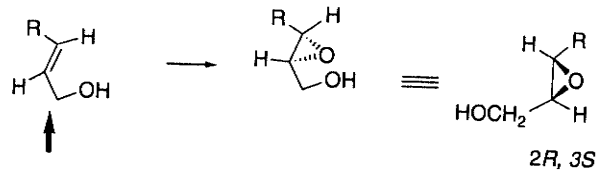

2R, 3S

2.29. (a) Classical resolution; (b) kinetic resolution; (c) chiral chromatography; (d) enantioselective synthesis.

2.30. The original reference analyzed the barrier in terms of σ-π hyperconjugation. However, as suggested by the analysis of ethane in Topic 1.1, the rotational barrier is affected by adjustments in molecular geometry, which will lead to changes in all components of the total energy. The analysis of the acetaldehyde rotational barrier given on p. 148 shows that nuclear-nuclear and electron-electron, and nuclear-electron interactions all contribute to the overall barrier.

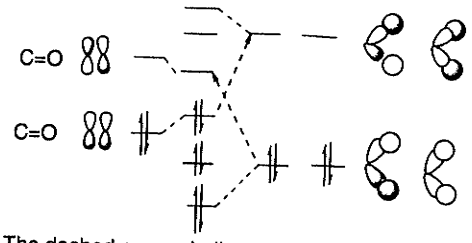

The dashed arrows indicate the attractive hyperconjugative interactions.

2.31. These observations can be accounted for by a rapid equilibration of the monochlorophosphonates, followed by diastereoselective reaction with 4-nitrophenol.

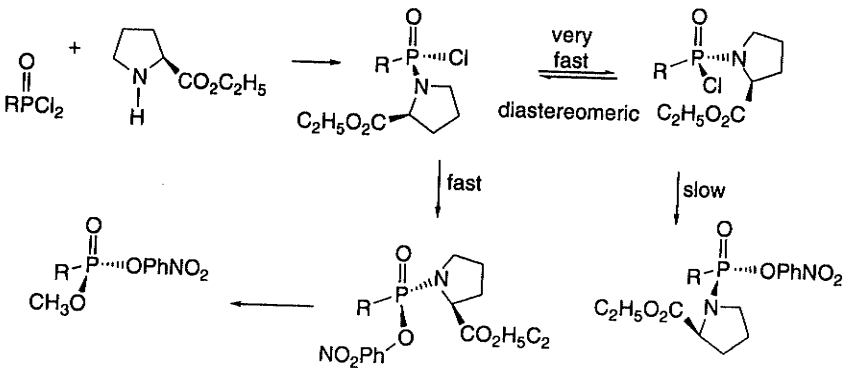

kinetic resolution is achieved at this stage of the reaction

2.32. In the cited reference the experimental ratios are reported to be 96:4; 99.5:0.5, and 99.9:0.1 This is in order of expectation of the steric interference with *endo* hydroboration. The complication is that the experimental values may include some hydroboration by the monoalkylborane, which would accentuate the steric factor.

2.33. The 1,3-dimethylcycloalkenes would be expected to have the 3-methyl substituent in a pseudoaxial position to avoid $A^{1,3}$ allylic strain. This directs the hydroboration to the opposite face. The *syn* addition then results in the formation of the *trans*, *trans*-2,6-dimethylcycloalkanol.

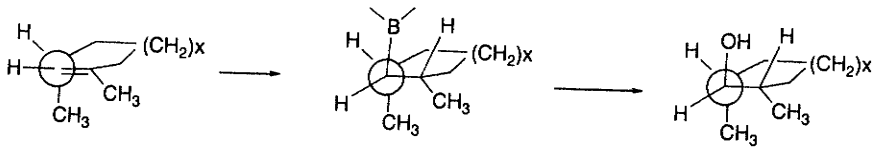

2.34. The stereoselectivity in the protected derivatives is governed by steric factors with the relatively large silyloxy group favoring hydrogenation from the opposite face. The Crabtree catalyst is known to be responsive to *syn*-directive effects by the hydroxy group. The noticeable decrease in stereoselectivity of the carbomethoxy derivative may be due to competing complexation at the ester carbonyl.

Chapter 3

3.1. a. The difference in ΔH_f between cyclohexene and cyclohexane gives the ΔH_{H2} for cyclohexene as 28.4 kcal/mol. A rough estimate of the heat of hydrogenation of cyclohexa-1,3,5-triene would be three times this value or 85.2 kcal/mol. The difference of 36.8 kcal/mol is an estimate of the stabilization of benzene relative to cyclohexa-1,3,5-triene. This estimate makes no allowance for the effect of conjugation in cyclohexa-1,3,5-triene, since it uses the isolated double bond cyclohexene as the model.

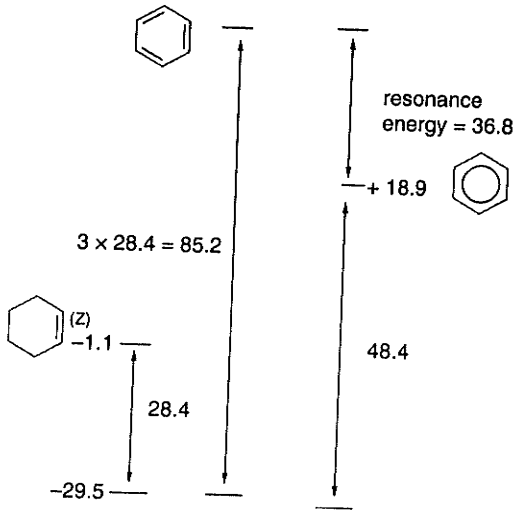

b. The enthalpy of oxidation can be obtained by a simple thermochemical calculation, since the ΔH_f for O_2, the element in its standard state, is 0.

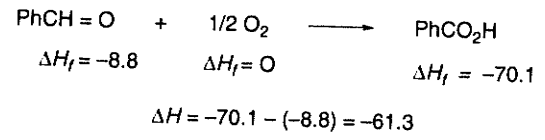

$$\Delta H = -70.1 - (-8.8) = -61.3$$

c. The difference in ΔH_f between 2-methyl-1-pentene and 2-methylpentane corresponds to the heat of hydrogenation.

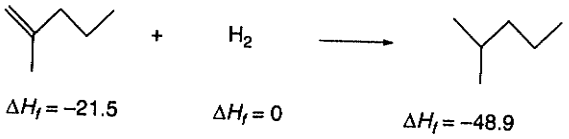

$$\Delta H_{H2} = -48.9 - (-21.5) = -27.4$$

3.2. These conditions would lead to an isomeric mixture of 1,2-dimethylcyclohexanol that would be dehydrated to the three alkenes shown.

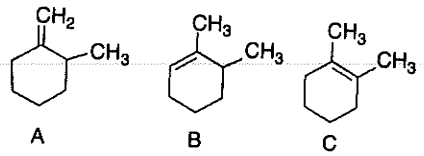

The formation of a stereoisomeric mixture of 1,2-dimethylcyclohexane from each is in accord with these assignments. The H^+-catalyzed equilibration would establish the thermodynamic equilibrium so that the structures can be assigned on the basis of relative stability. The relative stability of the alkenes should be C > B > A, based on the number of double-bond substituents.

3.3. A plot of ln K versus $1/T$ gives a good straight line with a slope of 2428. By use of Equation (3.1), this give $\Delta H = 4.80$ kcal/mol and $\Delta S = -12.2$ eu

Temp C	Temp K	1/Temp	K	Ln K	ΔG	ΔH	ΔS
−2.9	270.2	0.00370	16.9	2.827314	−1512.6	−4807.64	−12.1948
11.8	284.9	0.00351	11.0	2.397895	−1352.7	−4807.64	−12.1270
18.1	291.2	0.00343	8.4	2.128232	−1227.1	−4807.64	−12.2958
21.9	295.0	0.00340	7.9	2.066863	−1207.3	−4807.64	−12.2047
29.3	302.4	0.00331	6.5	1.871802	−1120.8	−4807.64	−12.1921
32	305.1	0.00328	6.1	1.808289	−1092.4	−4807.64	−12.1772
34.9	308.0	0.00325	5.7	1.740466	−1061.4	−4807.64	−12.1631
37.2	310.3	0.00322	5.3	1.667707	−1024.6	−4807.64	−12.1915
42.5	315.6	0.00317	4.6	1.526056	−953.61	−4807.64	−12.2117